

# Linear theory of gyro-traveling-wave-tubes with distributed losses

G. S. Nusinovich<sup>a)</sup> and O. V. Sinitsyn

*Institute for Plasma Research, University of Maryland, College Park, Maryland 20742*

A. Kesar

*Tel Aviv University, Ramat Aviv 69978, Israel*

(Received 21 February 2001; accepted 20 April 2001)

A small-signal theory describing two-stage gyro-traveling-wave tubes (gyro-TWTs) with the first stage having distributed losses is developed. In addition to the study of a small-signal gain in this device, the self-excitation conditions for parasitic backward waves are also analyzed. The theory is illustrated by using it for describing the performance of the gyro-TWT designed at the Naval Research Laboratory. The results show a very good agreement between the predictions of analytical theory and a thorough numerical analysis based on the use of well-developed codes. © 2001 American Institute of Physics. [DOI: 10.1063/1.1381423]

## I. INTRODUCTION

As is known, the studies of electromagnetic (EM) wave amplification in devices based on the cyclotron maser instability were started in the late 1950's<sup>1-3</sup> (see also reviews<sup>4,5</sup> for references). An active development of gyro-traveling-wave-tubes (gyro-TWT's) based on the above-mentioned instability began in the late 1970's.<sup>5-10</sup> During the 1990's these tubes were most actively developed at the Naval Research Laboratory (NRL),<sup>11</sup> the University of California (UC), Davis<sup>12</sup> and at the National Tsing Hua University (NTHU), Taiwan.<sup>13,14</sup> Recently the work at NTHU culminated in the development of Ka-band gyro-TWT with 70 dB gain and 3% bandwidth.<sup>15</sup> It was possible to realize such an ultra-high gain due to the use of distributed wall losses for the suppression of spurious oscillations. The impressive results achieved at NTHU stimulated the interest of NRL researchers in this concept: their design of a Ka-band gyro-TWT is presented in Ref. 16.

In spite of the presence of numerous experimental results and numerical simulations, a simple linear theory of a gyro-TWT, in which a part of the waveguide has finite losses,<sup>15,16</sup> has not been developed yet. (As a certain step towards this theory, Ref. 17 which analyzes a gyro-TWT with nonuniform distributed losses should be mentioned.)

In the present paper an attempt to develop such a theory is made. The paper is organized as follows. Section II contains the formalism describing a small-signal operation of the two-stage gyro-TWT, in which the first stage has distributed losses. In Sec. III the results of the gain and bandwidth studies are presented. In Sec. IV the backward wave excitation is considered. In Sec. V the theory is applied to the NRL gyro-TWT design.<sup>16</sup> Finally, Sec. VI contains a summary of results. In Appendices the relation between dispersion equations for the gyro-TWT and conventional TWT (Appendix A) and the operation at the grazing point (Appendix B) are discussed.

<sup>a)</sup>Electronic mail: gregoryn@glue.umd.edu

## II. GENERAL FORMALISM

Since the linear theory of multi-stage forward-wave amplifiers was recently considered in detail in Ref. 18, below we will outline only the most important steps in the derivation of the corresponding equations. We will consider the operation far enough from cutoff, when the nonsynchronous interaction of electrons with the backward wave can be neglected. We will also neglect the electron spread in velocities and guiding center radii and the space charge effects. Then, a corresponding self-consistent set of linearized equations can be written<sup>18</sup> as

$$\frac{d\tilde{w}}{d\zeta} = -\tilde{F}, \quad (1)$$

$$\frac{d\tilde{\theta}}{d\zeta} = (1 - b\Delta)\tilde{w} + \frac{s}{2i}\tilde{F}, \quad (2)$$

$$\frac{d\tilde{F}}{d\zeta} - i\Delta\tilde{F} = -I_0 \left\{ i\tilde{\theta} - \left( \frac{s}{2} - b \right) \tilde{w} \right\}. \quad (3)$$

Here  $\tilde{w}$  and  $\tilde{\theta}$  are perturbations in slowly variable electron energy and phase averaged over initial electron phases, respectively;  $\tilde{F}$  is the wave amplitude normalized to the input wave amplitude  $F_0$  (so  $\tilde{w}$  and  $\tilde{\theta}$  are also normalized to  $F_0$ ),  $\zeta$  is the normalized axial coordinate,  $s$  is the cyclotron resonance harmonic number, parameter  $b$  characterizes the changes in the electron axial velocity with the change in electron energy and  $I_0$  is the normalized beam current parameter given elsewhere.<sup>18-21</sup>

$$I_0 = 16 \frac{eI_b}{mc^3} \frac{1}{h\kappa^2} \frac{(1 - h\beta_{z0})^3}{\gamma_0\beta_{\perp 0}^4} \left[ \frac{\alpha^{s-1}}{(s-1)!2^s} \right]^2 G_{\text{cpl}}.$$

Here  $I_b$  is the beam current,  $\beta_{\perp 0}$  and  $\beta_{z0}$  are, respectively, the initial orbital and axial electron velocities normalized to the speed of light and  $h = k_z/(\omega/c)$  and  $\kappa = k_{\perp}/(\omega/c)$  are the normalized axial and transverse wavenumbers, respectively. Also  $\alpha = k_{\perp}r_L \approx s\kappa\beta_{\perp 0}/(1 - h\beta_{z0})$  is the normalized Larmor radius and  $G_{\text{cpl}}$  is the coupling im-

pedance, which for a thin annular electron beam in a cylindrical waveguide is equal to  $J_{m\mp s}^2(k_\perp R_0)/(\nu^2 - m^2)J_m^2(\nu)$ . Here  $\nu = k_\perp R_w$  ( $R_w$  is the waveguide radius) is the  $p$ -th root of the equation  $J'_m(\nu) = 0$  for the  $TE_{m,p}$ -wave.

In Eqs. (2)–(3)  $\Delta$  is the normalized cyclotron resonance mismatch between the Doppler-shifted wave frequency  $\omega - k_z v_{z0}$  and the resonant harmonic of the electron cyclotron frequency  $s\Omega_0$ :  $\Delta \sim \omega - k_z v_{z0} - s\Omega_0$ . Therefore, in the waveguide section with distributed losses  $k_z$ , and correspondingly  $\Delta$ , are complex, while in the lossless section  $k$  and  $\Delta$  are real. When the operating voltage and the axial wavenumber are not too large,  $\Delta \approx (2/\beta_{\perp 0}^2)(1 - h\beta_{z0} - s\Omega_0/\omega)$ . (The above-mentioned assumptions correspond to  $h^2$ ,  $h\beta_{z0} \ll 1$ .) Correspondingly, the imaginary part of  $\Delta$ , which is responsible for losses, is equal to  $d = (2\beta_{z0}/\beta_{\perp 0}^2)h''$  where  $h'' = ck_z''/\omega$ . The normalized axial coordinate is  $\zeta = (\beta_{\perp 0}^2/2\beta_{z0})(\omega z/c)$ , so the product of  $d$  and  $\zeta$  is just  $k_z''z$ .

As is known,<sup>19–21</sup> considering perturbations  $\tilde{w}$ ,  $\tilde{\theta}$  and  $\tilde{F}$  to be proportional to  $\exp(i\Gamma\zeta)$  yields the cubic dispersion equation for propagation constants  $\Gamma$ :

$$(\Gamma - \Delta)(\Gamma^2 + I_0 b) - sI_0 \Gamma + I_0 = 0. \quad (4)$$

Recall that, first, at small values of the beam current parameter  $I_0$ , this equation can be reduced<sup>22</sup> to the standard dispersion equation for linear-beam TWTs:<sup>23</sup>

$$\gamma^2(\gamma - \delta) + 1 = 0. \quad (5)$$

[In Eq. (5)  $\gamma = \Gamma/I_0^{1/3}$  and  $\delta = \Delta/I_0^{1/3}$ , the relation between parameters used in the theory of gyro-TWTs and linear-beam TWTs is given in Appendix A.] Second, this cubic dispersion equation can also be obtained from the original fourth-order dispersion equation<sup>24–27</sup> in which the interaction with the backward wave is not ignored (this equation is discussed in Appendix B).

So, perturbations  $\tilde{w}$ ,  $\tilde{\theta}$  and  $\tilde{F}$  can be represented<sup>18</sup> as

$$\begin{aligned} \tilde{w} &= i \sum_{l=1}^3 \frac{C_l}{\Gamma_l} e^{i\Gamma_l \zeta}, & \tilde{\theta} &= \sum_{l=1}^3 \frac{C_l}{\Gamma_l} \left[ (1 - b\Delta) \frac{1}{\Gamma_l} - \frac{s}{2} \right] e^{i\Gamma_l \zeta}, \\ \tilde{F} &= \sum_{l=1}^3 C_l e^{i\Gamma_l \zeta}. \end{aligned} \quad (6)$$

Here  $\Gamma_l$  are the roots of Eq. (4) and  $C_l$  are the coefficients, which should be determined by the boundary conditions.

For the first stage of the device, the absence of modulation in electron energies and phases at the entrance, as well as the presence of the input wave, yield the following boundary conditions (cf. Ref. 18):

$$\sum_{l=1}^3 C_l = 1, \quad \sum_{l=1}^3 \frac{C_l}{\Gamma_l} = 0, \quad \sum_{l=1}^3 \left( 1 - b\Delta - \frac{s}{2}\Gamma_l \right) \frac{C_l}{\Gamma_l^2} = 0. \quad (7)$$

The first two equations here are the same as in the theory of the linear-beam TWT,<sup>23</sup> while the last one is more complicated because, as follows from Eq. (2), the phase perturbation depends not only on the energy perturbation (as in con-

ventional TWT's) but also on the changes in the electron axial velocity and on the direct action of the wave field on the phase.

After calculating the coefficients  $C_l$  determined by Eqs. (7) one can find, by using Eqs. (6), the electron energy and phase and the wave amplitude at the end of the first stage. These values then should be used as the boundary conditions for the same variables at the entrance to the second stage. Below we will neglect the wave reflection at this interface. Recall that the propagation constants  $\Gamma_l$  for the second, lossless waveguide section should be found from the dispersion equation (4) with the real mismatch  $\Delta$ . Correspondingly, the gain of such a two-stage gyro-TWT can be determined as  $G = G_1 + G_2$  where

$$G_1 = 20 \log \left\{ \left| \sum_{l=1}^3 C_l^{(I)} e^{i\Gamma_l^{(I)} \zeta_{\text{out}}^{(I)}} \right| \right\} \quad (8)$$

is the gain of the first stage of the length  $\zeta_{\text{out}}^{(I)}$  and

$$G_2 = 20 \log \left\{ \left| \sum_{l=1}^3 C_l^{(II)} e^{i\Gamma_l^{(II)} (\zeta_{\text{out}} - \zeta_{\text{out}}^{(I)})} \right| \right\} \quad (9)$$

is the gain of the second stage in the device of a total length  $\zeta_{\text{out}}$ . Roman indices I and II designate here the first and second stages, respectively, for which the propagation constants  $\Gamma_l$  and coefficients  $C_l$  should be calculated separately, as discussed above.

### III. RESULTS

Our study was focused on the effect of distributed losses on the gain and bandwidth of the two-stage gyro-TWT. Before starting to consider the effect of significant losses, let us consider analytically the effect of small losses. This is the case when the complex detuning  $\Delta$  can be represented as  $\Delta' + id$  and the loss parameter  $d$  can be treated as a small parameter in the dispersion equation (4). Such a treatment was done for the case of exact synchronism between electrons and the wave in the linear-beam TWT in Ref. 23 and in the gyro-TWT in Ref. 26. (Note that in the latter paper the condition of exact synchronism was called the grazing condition.) The important conclusion from this treatment was that for small losses the reduction in the gain of the growing wave from the gain in dB for zero loss is 1/3 of the circuit attenuation in dB. For TWT's this statement, being expressed in terms of  $\text{Im } \gamma$  [recall that for  $\exp(i\gamma\zeta)$  perturbations the growing wave has  $\text{Im } \gamma < 0$ ], can be written as

$$|\text{Im } \gamma| = |\text{Im } \gamma_{(0)}| - \frac{1}{3} d_{\text{TWT}}. \quad (10)$$

Here  $\gamma_{(0)}$  is the solution which follows from Eq. (5) when  $\delta' = d = 0$  ( $\delta'$  is the real part of the detuning); the loss parameter  $d_{\text{TWT}}$  relates to the gyro-TWT loss parameter  $d$  as  $d_{\text{TWT}} = d/I_0^{1/3}$ .

In order to estimate this effect in a certain frequency band, we carried out a similar analysis for nonzero detunings, i.e., we considered

$$\gamma = \gamma_{(0)}(\delta') - d_{\text{TWT}} \gamma_{(1)}(\delta'). \quad (11)$$

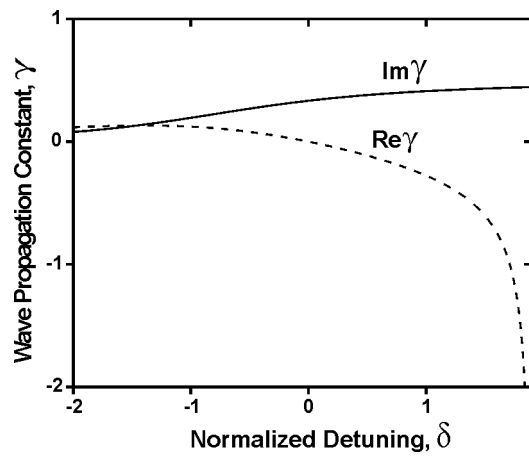


FIG. 1. First-order corrections to real and imaginary parts of propagation constants (for the case of small losses) as functions of the normalized cyclotron resonance detuning.

Here  $\gamma_{(0)}(\delta')$  is the solution of Eq. (5) for  $d=0$  but nonzero  $\delta'$ , which can be found elsewhere,<sup>23</sup> and  $\gamma_{(1)}(\delta')$  is the solution of the first-order equation, which follows from Eq. (5). Both, real and imaginary parts of  $\gamma_{(1)}$  as functions of the detuning  $\delta$  (the prime is omitted below) are shown in Fig. 1. As is seen in Fig. 1, at  $\delta=0$   $\text{Im } \gamma_{(1)}=1/3$ , which corresponds to known results,<sup>23,26</sup> at positive  $\delta$ 's, where the efficiency is higher,<sup>21</sup> the effect of losses on the growth rate is a little stronger. Taking into account that, at least, up to  $I_0=0.1$  the solution of Eq. (4) is close enough to that of Eq. (5),<sup>28</sup> one should expect from solving Eq. (4) results similar to those shown in Fig. 1.

For finite values of the loss parameter  $d$  Eq. (4) was solved numerically. (It was assumed here and below that  $b \rightarrow 0$ .) Corresponding imaginary parts of the complex roots  $\Gamma$  are shown as functions of the detuning  $\Delta$  for several values of  $d$  in Fig. 2. Here Figs. 2(a) and 2(b) correspond to the normalized beam current parameter values 0.03 and 0.3, respectively. Note, that these results are quite similar to those for conventional TWTs shown in Figs. 8.1–8.3 in Ref. 23. From the results shown it follows that losses decrease the maximum growth rate of the wave but, at the same time, increase the range of resonance detunings, in which the wave amplification is possible. (The latter conclusion was also made in Refs. 16 and 26.)

Since the losses simultaneously decrease the gain and increase the bandwidth, it is interesting to check how the losses affect the gain bandwidth product, which is the figure-of-merit of microwave sources for various applications. (To the best of our knowledge, such an analysis has not been done previously.) To estimate the effect of the losses on the gain-bandwidth product, let us compare results shown in Figs. 3(a) and 3(b). In both figures the gain as the function of detuning  $\Delta$  is shown for the same beam current parameter  $I_0=0.3$  and several lengths of the waveguide,  $\zeta_{\text{out}}$ . Figure 3(b) corresponds to the case when the first waveguide stage has the normalized length  $\zeta_{\text{out}}^{(1)}=5$  and the loss parameter  $d=0.3$ . So the total length in both cases is the same for corresponding curves shown in Figs. 3(a) and 3(b). The comparison allows us to conclude that the given losses decrease

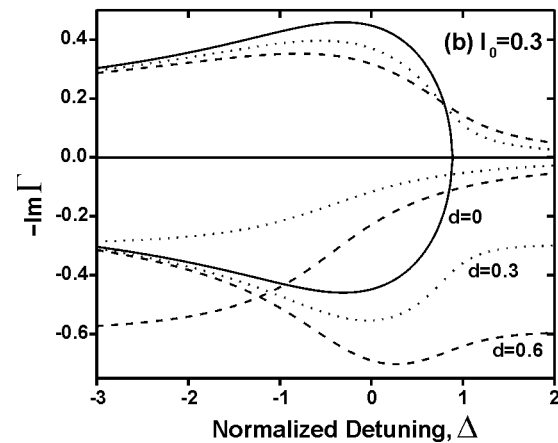
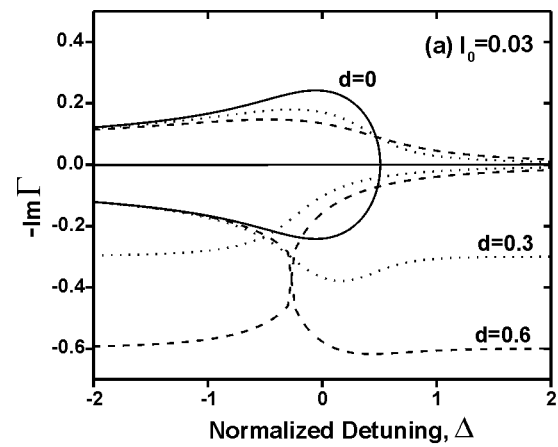


FIG. 2. An imaginary part of propagation constants as the function of the normalized detuning for several values of the loss parameter  $d$  and small (a)  $I_0=0.03$  and large (b)  $I_0=0.3$  values of the normalized beam current parameter.

the total gain by less than 3 dB and simultaneously increase the range of  $\Delta$ 's at the  $-3$  dB level by 20% and more. Correspondingly, in the case of the bandwidth expressed in terms of  $\Delta$ 's, it means that the losses increase the gain-bandwidth product by about 10%. Bearing in mind that the relation between the real frequency bandwidth and corresponding range of detunings  $\Delta$  depends on the operating point (as shown in Ref. 28, at the grazing point the frequency deviation does not affect  $\Delta$  at all), we would like to emphasize here that our results show only that an enhancement of the gain-bandwidth product due to distributed losses is possible, in principle. Concrete estimates will be made below.

#### IV. BACKWARD-WAVE EXCITATION

A parasitic excitation of backward waves is the most critical issue in the development of high-gain gyro-TWTs.<sup>14–16</sup> Since it is preferable to have an amplifier which operates stably even in the absence of the signal, below we will study the start of oscillation conditions in our two-stage gyro-TWT in the absence of forward waves. In this study we describe a so-called zero-drive stability of the device. (The effect of the forward wave on the starting current of backward wave oscillations was recently analyzed in Ref. 29.)

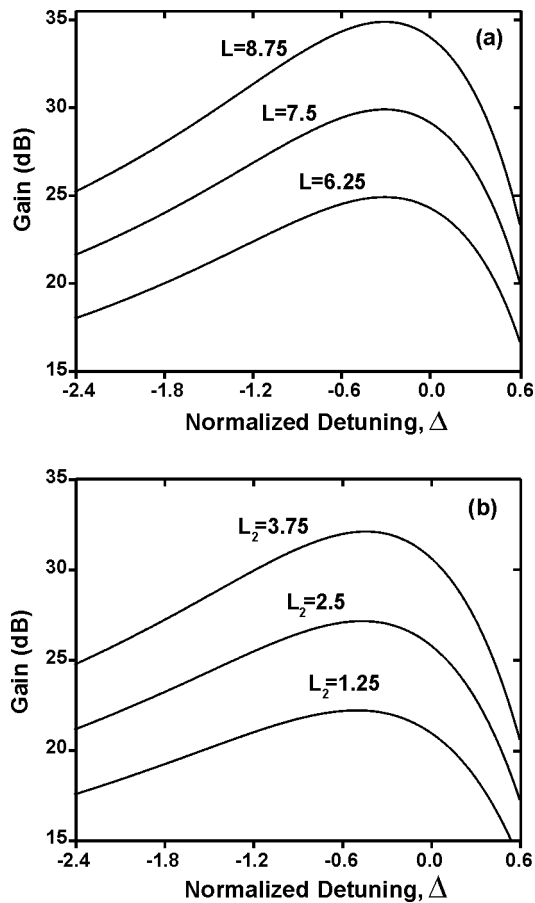


FIG. 3. The gain as the function of the normalized cyclotron resonance detuning for  $I_0=0.3$  and several values of the interaction length: (a) lossless waveguide, its total length is given in the figure; (b) the first section of the length  $L_1=5$  has the loss parameter  $d=0.3$ ; the length of the second section is given in the figure.

In general, a similarity of the dispersion equation for gyro-backward-wave oscillators (gyro-BWO's) to that for linear beam BWO's allows one to study the starting conditions in gyro-BWO's by the methods known for conventional BWO's.<sup>30</sup> Such a method was used for analyzing the starting conditions in single-stage gyro-BWO's elsewhere.<sup>31,32</sup> (The case of mismatched boundary conditions for the wave was considered in Ref. 33.)

We applied the same formalism for studying a two-stage gyro-BWO with the first section having distributed losses. As above, it was assumed that the values of the electron energy and phase and the wave amplitude at the end of the first stage can be used as the boundary conditions for corresponding variables in the second stage. Recall that in the case of backward-wave interaction two last terms in the dispersion equation, Eq. (4), have opposite signs<sup>19</sup> because parameters  $I_0$  and  $b$  change their signs. The results of calculations are presented in Fig. 4 as the dependencies of the length of the second stage, at which the self-excitation starts, on the loss parameter  $d$  for several values of the normalized current parameter  $I_0$  and several lengths of the first stage. In Fig. 4 solid, dashed and dotted lines correspond to the normalized length of the first stage equal to 5, 10 and 15, respectively. As is seen in Fig. 4, when the losses are small the

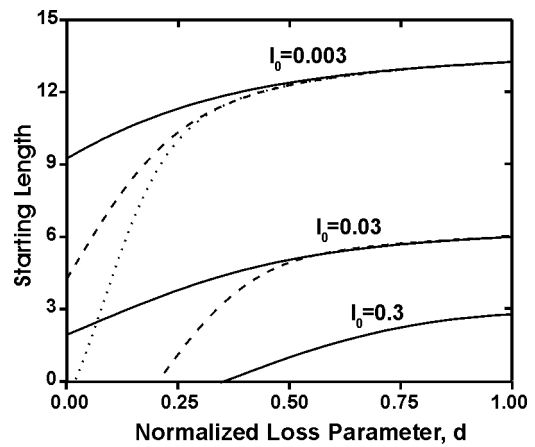


FIG. 4. BWO self-excitation conditions: the starting length of the second section is shown as the function of loss parameter  $d$  for several values of the normalized beam current and different lengths of the first section (solid, dashed and dotted lines correspond to  $L_1=5, 10$  and  $15$ , respectively).

starting length of the second stage strongly depends on the length of the first stage. However, starting from the loss parameter values  $d \approx 0.5$ , the length of the first stage does not play any role. This indicates that the first stage becomes so lossy that the oscillations appear just in the second, lossless stage.

The results illustrating the effect of losses on the self-excitation of the first section are shown in Fig. 5. Here the starting length of a single-stage gyro-BWO is shown as the function of losses for several values of the normalized current parameter. As is seen, for any value of the current there is a critical value of the losses, above which the self-excitation is impossible for any length. This is the case when the attenuation rate caused by losses is larger than the beam-induced growth rate of the wave.

V. ANALYSIS OF THE NRL-GYRO-TWT

Let us now illustrate the general treatment given above by considering a Ka-band gyro-TWT designed at NRL.<sup>16</sup> This tube is driven by a 70 kV, 6 A electron beam with the orbital-to-axial velocity ratio of about 0.71. The interaction circuit is a circular waveguide of 2.72 mm radius and of a 27

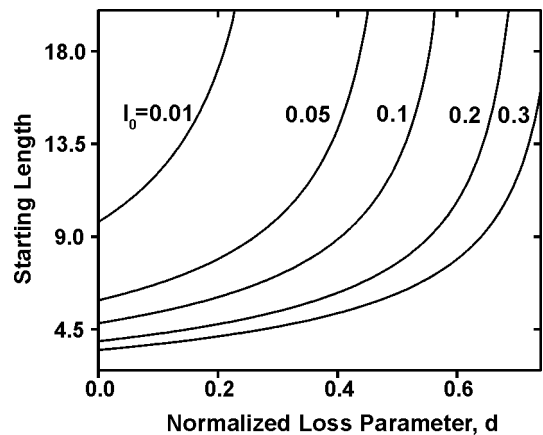


FIG. 5. The starting length of a lossy waveguide as the function of the loss parameter  $d$  for several values of the normalized beam current.

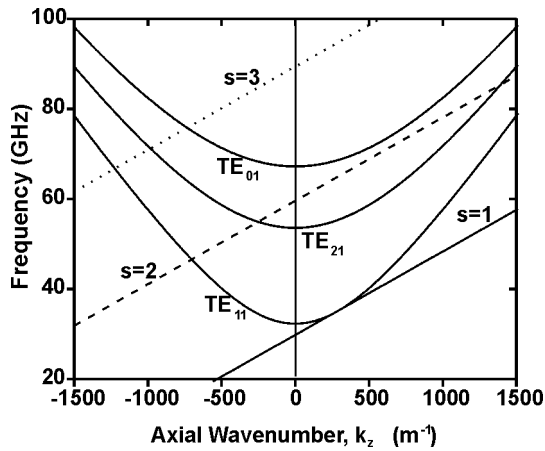


FIG. 6. Dispersion diagram for the operating  $TE_{11}$ -wave and spurious  $TE_{21}$ - and  $TE_{01}$ -waves for the gyro-TWT design.<sup>16</sup>

cm total length. The first 22 cm of this waveguide have cold circuit losses of 3.45 dB/cm, which for the central frequency 35 GHz corresponds to the loss parameter  $d=0.553$ , and the last 5 cm are free of losses. The operating mode is the  $TE_{11}$ -wave. The dispersion curve for this mode and two parasitic waves are shown in Fig. 6; there are also shown the cyclotron beam lines for the resonances at first three cyclotron harmonics ( $s=1, 2$  and 3). The case of grazing for the operating wave at the fundamental resonance, which is shown in Fig. 6, corresponds to the external magnetic field  $B_0=12.08$  kG.

As is seen in Fig. 6, in the region of backward-wave interaction, the  $TE_{21}$ -wave can be excited closer to cutoff than other modes; so one can expect that this wave is the most troublesome parasite. Indeed, the analysis of backward-wave self-excitation conditions showed that for this mode the normalized beam current parameter  $I_0$  is equal to 0.0137 and the normalized lengths of the first and second waveguide sections are equal to 26 and 5.92, respectively; at the same time the starting length of the second, lossless section is equal to 7.3, i.e., exceeds the real length by about 20% only. For the backward  $TE_{11}$ -wave at the second cyclotron harmonic the normalized lengths of two sections are equal to 14.0 and 3.2; and the normalized beam current parameter is 0.0029 only. Correspondingly, the starting length of the second section is about 14.0; so there are huge safety margins.

As it was mentioned in Sec. III, to correctly evaluate the bandwidth of the device one should know the relation between the normalized detuning of the cyclotron resonance  $\Delta$  and the wave frequency. This dependence is shown in Fig. 7(a) for several values of the external magnetic field  $B_0$  in terms of its ratio to the grazing value  $B_g$ . Note that, although Fig. 3 given above demonstrates a significant gain at both positive and negative detunings  $\Delta$ , nonlinear calculations presented elsewhere<sup>21</sup> predict a high efficiency at positive  $\Delta$ 's only. This indicates that, as follows from Fig. 7(a), it is preferable to operate at magnetic fields equal or slightly below the grazing value. Figure 7(b) shows the dependence of the normalized beam current of the operating wave  $I_0$  on the operating frequency. As the frequency increases, the wave group velocity increases as well, and correspondingly, the

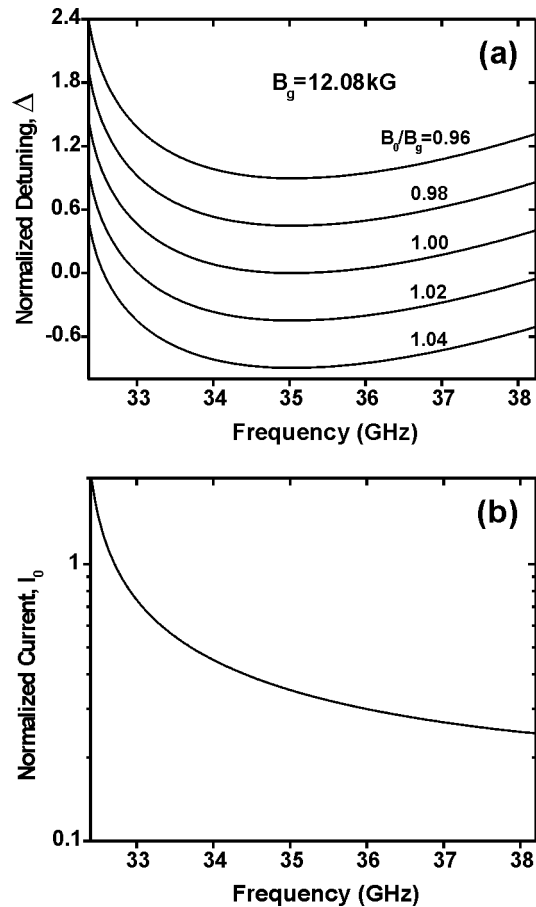


FIG. 7. (a) Dependence of the normalized detuning  $\Delta$  on the operating frequency for several values of the external magnetic field; (b) normalized beam current parameter of the operating  $TE_{11}$ -wave as the function of frequency.

beam current parameter  $I_0$  becomes smaller. In spite of this increase, in all the frequency range shown its value exceeds the normalized current of the most dangerous parasitic  $TE_{21}$ -wave by more than an order of magnitude.

The resulting gain calculated in accordance with Eqs. (8) and (9) is shown in Fig. 8. As follows from this figure, the

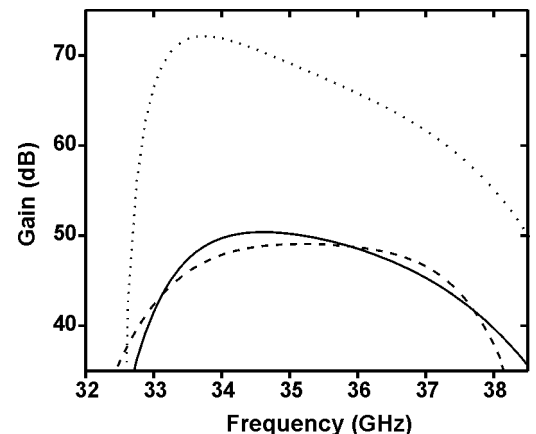


FIG. 8. Gain as the function of frequency for the NRL gyro-TWT design (Ref. 16). The results of Ref. 16 are shown by the dashed line. The dotted line shows the lossless gyro-TWT results.

bandwidth at the  $-3$  dB level is about 3 GHz and the maximum gain is about 50 dB. For the sake of comparison, there are also presented in Fig. 8 by a dashed line the design data, which correspond to calculations of the output power for a small value of the input power,  $P_{\text{in}}=0.9$  W (see Fig. 12 in Ref. 16), which is the case closest to the small-signal operation. As is seen, there is a good agreement between the gains calculated by the two methods. The gain found in Ref. 16 is a little smaller, possibly, first, due to the effect of 4% velocity spread and second, because at  $P_{\text{in}}=0.9$  W we can already observe in Fig. 11 of Ref. 16 some saturation effects. The fact that the bandwidth calculated in Ref. 16 is a little larger (about 3.6 GHz) than that found in our simulations, can be attributed to the down-taper of the external magnetic field in the region of the lossless waveguide, which we ignored in our theory. (Note that this taper, as is shown in Fig. 10 of Ref. 16 and discussed in its text, may even cause the appearance of the second peak in the dependence of the output power upon the operating frequency.)

In Fig. 8 the dotted line shows the small-signal gain in the lossless gyro-TWT of the same length. Certainly, the gain is much higher: as follows from Fig. 8, the maximum gain in the presence of losses is about 2/3 of that for a lossless gyro-TWT. (Recall that the backward wave excitation occurs in a lossless tube of such a length.) However, the gain-bandwidth product in the tube with losses exceeds its value in a lossless counterpart by more than 10%. This agrees well with the results of Sec. III.

## VI. SUMMARY

A small-signal theory of two-stage gyro-TWTs with the first stage having some distributed losses is developed. Also the analysis of self-excitation conditions for spurious backward oscillations is carried out. An example is considered which shows that predictions of this simple analytical theory may agree well with the results of a thorough numerical analysis based on the use of accurate codes.

In conclusion, let us note that our formalism was focused on two-stage gyro-TWTs because just such gyro-TWT configurations are currently under development at various laboratories. This formalism can easily be generalized on the case of three-stage gyro-TWTs with a central lossy section. Recall that in the past such configurations of linear-beam TWTs were actively developed.

## ACKNOWLEDGMENT

This work is done in the framework of a Multidisciplinary University Research Initiative (MURI) on innovative vacuum electronics sponsored by the Air Force Office of Scientific Research.

## APPENDIX A: RELATION BETWEEN THE DISPERSION EQUATIONS FOR THE GYRO-TWT AND LINEAR-BEAM TWT

As shown in Ref. 22, the approximate dispersion equation for the gyro-TWT can be written as

$$k_z - k_{z0} = \frac{1}{(\omega - k_z v_{z0} - s\Omega_0)^2} \left( -\frac{eI_b}{mv_{z0}N} \right) \times \{ |G_{zs}|^2 (1 - \beta_{z0}^2) - |G_{\theta s}|^2 \beta_{\perp 0}^2 - (G_{\theta s} G_{zs}^* + G_{\theta s}^* G_{zs}) \beta_{\perp 0} \beta_{z0} \}. \quad (\text{A1})$$

Here  $k_z$  and  $k_{z0}$  are the axial wavenumbers in the presence and absence of an electron beam, respectively. Also  $N$  is the norm of the wave and  $G_{zs}$  and  $G_{\theta s}$  are, respectively, the axial and azimuthal components of the Lorentz force acting on electrons in the case of cyclotron resonance at the  $s$ -th harmonics. Assuming that the beam perturbs the axial wavenumber only slightly and that the operation is close to the cyclotron resonance condition, we can introduce small mismatches  $\delta$  and  $\varepsilon$  ( $|\delta|, |\varepsilon| \ll 1$ ) by

$$k_z - k_{z0} = \delta k_{z0}$$

and

$$\omega - k_{z0} v_{z0} - s\Omega_0 = \varepsilon k_{z0} v_{z0}$$

and rewrite Eq. (A1) as

$$\delta(\varepsilon - \delta)^2 = -\frac{eI_b}{mc^3} \frac{\omega}{\beta_{z0}^3 k_{z0}^3 N} \times \{ |G_{zs}|^2 (1 - \beta_{z0}^2) - \beta_{\perp 0}^2 |G_{\theta s}|^2 - \beta_{z0} \beta_{\perp 0} (G_{\theta s} G_{zs}^* + G_{\theta s}^* G_{zs}) \}. \quad (\text{A2})$$

Introducing  $\Gamma = \varepsilon - \delta$  and  $\hat{I} = (eI_b/mc^3)(\omega/\beta_{z0}^3 k_{z0}^3 N)$ , allows us to rewrite Eq. (A2) as

$$\Gamma^2(\Gamma - \varepsilon) - \hat{I} \{ |G_{zs}|^2 (1 - \beta_{z0}^2) - \beta_{\perp 0}^2 |G_{\theta s}|^2 - \beta_{z0} \beta_{\perp 0} (G_{\theta s} G_{zs}^* + G_{\theta s}^* G_{zs}) \} = 0. \quad (\text{A3})$$

In the case of the gyro-TWT operating in a TE-mode, as shown in Ref. 34, the expression in figure brackets can be reduced to  $-\beta_{\perp 0}^2 [(\omega/c)^2 - k_z^2] |(\nabla_{\perp} \Psi_s)_r|^2$  where  $\Psi_s$  is the membrane function describing the transverse structure of the operating mode. So, bearing in mind that  $\varepsilon$  characterizes the cyclotron resonance mismatch, one can easily reduce Eq. (A3) to Eq. (5).

In the case of the linear-beam TWT we should, first, consider a TM-wave, and second, assume  $\beta_{\perp 0} = 0$ . Then, we should recall that in this case the cyclotron harmonic number  $s$  is equal to zero, so  $\varepsilon$  is proportional to  $v_{\text{ph}} - v_{z0}$ , while the Pierce parameter  $b^{23}$  is proportional to  $v_{z0} - v_{\text{ph}}$ . Also, Pierce considered perturbations in the form  $e^{i\omega t - \Gamma z}$ , which corresponds to  $e^{C\delta k_{z0} z}$  in his notations, while our perturbations are presented as  $e^{i(\omega t - k_z z)} \sim e^{-i\delta k_{z0} z} \sim e^{i\Gamma k_{z0} z}$ . So, our  $i\Gamma$  corresponds to Pierce's  $C\delta$ . With all this in mind one can reduce Eq. (A3) to

$$\delta^2 = \frac{1}{i\delta - b + id}, \quad (\text{A4})$$

which is Eq. (7.14) from Ref. 23 for the case of negligibly small space-charge effects.

## APPENDIX B: WAVE AMPLIFICATION AT THE GRAZING POINT

The dispersion equation describing the cyclotron maser instability has been derived and studied in many papers.<sup>24–27</sup> In particular, in Ref. 25, with the use of this equation, the absolute instability was analyzed and the conclusion was made that the maximum growth rate occurs in the case of operation at the grazing point, which is the case when the wave group velocity  $v_{gr} = d\omega/dk_z = c^2/v_{ph} = c^2 k_z/\omega$  is equal to the electron axial velocity  $v_z$ . This conclusion was later interpreted as the condition for the maximum spatial growth rate of the wave. Below we would like to show that such a conclusion is wrong, although, of course, the operation near the grazing is preferable for a number of other reasons (e.g., large bandwidth).

Let us present the fourth-order dispersion equation, which was originally derived in Ref. 24 for electromagnetic perturbations propagating in the transversely homogeneous magnetoactive plasma along the external magnetic field:

$$n^2\omega^2 - c^2k^2 = \omega_b^2 \frac{\omega - kv_{z0}}{\omega - kv_{z0} \mp \Omega_0} + \omega_b^2 \frac{\beta_{\perp 0}^2}{2} \frac{c^2k^2 - \omega^2}{(\omega - kv_{z0} \mp \Omega_0)^2}. \quad (\text{B1})$$

Here  $n = c/v_{ph}$  is the refractive index of the medium, in which the wave propagates, and  $\omega_b$  is the beam plasma frequency. Below we will assume that we operate close enough to the exact cyclotron resonance, and hence, the first term on the right-hand side (rhs) of Eq. (B1) can be neglected.

In the case of convective instability, one can present the axial wavenumber  $k$  as  $h(1 + \nu)$  where  $h = \pm(\omega n/c)$ . Then, assuming that  $\omega - hv_{z0} \mp \Omega_0 = 0$ , one can readily reduce Eq. (B1) to

$$\nu^3 = \frac{\beta_{\perp 0}^2}{4\beta_{z0}^2} \frac{\omega_b^2}{\omega^2} \frac{1 - n^2}{n^4}. \quad (\text{B2})$$

Equation (B2) clearly shows that the spatial growth rate monotonically increases when the operating point approaches the cutoff ( $n \sim k_z$ ), so there is no extremum at the grazing point, which would correspond to  $n = \beta_{z0}$ . Also note that in real devices  $\omega_b^2 \sim I_b$ , and therefore, the growth rate given by Eq. (B2) is proportional to  $I_b^{1/3}$  as in all TWT's and gyro-TWT's. Last, recall that Eq. (B2) is not valid for the luminous waves, which propagate with  $v_{ph} = c$  (i.e.,  $n = 1$ ), because in this case the orbital and axial bunching cancel each other<sup>34–36</sup> [see also the comment to Eq. (A3)]. Therefore the last term on the rhs of Eq. (B1) vanishes, so the first

one should be kept. As known,<sup>4</sup> this term is responsible for M-type effects in cyclotron resonance masers (CRMs).

- <sup>1</sup>R. Q. Twiss, *Aust. J. Phys.* **11**, 567 (1958).
- <sup>2</sup>J. Schneider, *Phys. Rev. Lett.* **2**, 504 (1959).
- <sup>3</sup>A. V. Gaponov, *Izv. Vyssh. Uchebn. Zaved. Radiofiz.* **2**, 836 (1959).
- <sup>4</sup>A. V. Gaponov, M. I. Petelin, and V. K. Yulpatov, *Radiophys. Quantum Electron.* **10**, 794 (1967).
- <sup>5</sup>V. L. Granatstein, B. Levush, B. G. Danly, and R. K. Parker, *IEEE Trans. Plasma Sci.* **25**, 1322 (1997).
- <sup>6</sup>J. L. Sefor, V. L. Granatstein, K. R. Chu, P. Sprangle, and M. E. Read, *IEEE J. Quantum Electron.* **QE-15**, 848 (1979).
- <sup>7</sup>K. R. Chu, A. T. Drobot, V. L. Granatstein, and J. L. Sefor, *IEEE Trans. Microwave Theory Tech.* **MTT-27**, 178 (1979).
- <sup>8</sup>K. R. Chu, A. T. Drobot, H. H. Szu, and P. Sprangle, *IEEE Trans. Microwave Theory Tech.* **MTT-28**, 313 (1980).
- <sup>9</sup>Y. Y. Lau, K. R. Chu, L. R. Barnett, and V. L. Granatstein, *Int. J. Infrared Millim. Waves* **2**, 373 (1981).
- <sup>10</sup>P. E. Ferguson, G. Valier, and R. S. Symons, *IEEE Trans. Microwave Theory Tech.* **MTT-29**, 794 (1981).
- <sup>11</sup>G. S. Park, J. J. Choi, S. Y. Park, C. M. Armstrong, A. K. Ganguly, R. H. Kyser, and R. K. Parker, *Phys. Rev. Lett.* **74**, 2399 (1995).
- <sup>12</sup>Q. S. Wang, D. B. McDermott, and N. C. Luhmann, Jr., *IEEE Trans. Plasma Sci.* **24**, 700 (1996).
- <sup>13</sup>L. R. Barnett, L. H. Chang, H. Y. Chen, K. R. Chu, W. K. Lau, and C. C. Tu, *Phys. Rev. Lett.* **63**, 1062 (1989).
- <sup>14</sup>K. R. Chu, L. R. Barnett, H. Y. Chen, S. H. Chen, Ch. Wang, Y. S. Yeh, Y. C. Tsai, T. T. Yang, and T. Y. Dawn, *Phys. Rev. Lett.* **74**, 1103 (1995).
- <sup>15</sup>K. R. Chu, H. Y. Chen, C. L. Hung, T. H. Chang, L. R. Barnett, S. H. Chen, T. T. Yang, and D. J. Dialectis, *IEEE Trans. Plasma Sci.* **27**, 391 (1999).
- <sup>16</sup>K. T. Nguyen, J. P. Calame, D. E. Pershing, B. G. Danly, M. Garven, B. Levush, and T. M. Antonsen, Jr., *IEEE Trans. Electron Devices* **48**, 108 (2001).
- <sup>17</sup>T. J. Wu and C. S. Kou, *Int. J. Infrared Millim. Waves* **20**, 1353 (1999).
- <sup>18</sup>G. S. Nusinovich and M. Walter, *Phys. Rev. E* **60**, 4811 (1999).
- <sup>19</sup>V. L. Bratman, N. S. Ginzburg, G. S. Nusinovich, M. I. Petelin, and P. S. Strelkov, *Int. J. Electron.* **51**, 541 (1981).
- <sup>20</sup>A. W. Fliflet, *Int. J. Electron.* **61**, 1049 (1986).
- <sup>21</sup>G. S. Nusinovich and H. Li, *Int. J. Electron.* **72**, 895 (1992).
- <sup>22</sup>A. V. Gaponov, *Izv. Vyssh. Uchebn. Zaved. Radiofiz.* **4**, 547 (1961).
- <sup>23</sup>J. R. Pierce, *Traveling-Wave Tubes* (Van Nostrand, Toronto, 1950), p. 118.
- <sup>24</sup>V. V. Zheleznyakov, *Izv. Vyssh. Uchebn. Zaved. Radiofiz.* **3**, 57 (1960).
- <sup>25</sup>P. Sprangle and A. T. Drobot, *IEEE Trans. Microwave Theory Tech.* **MTT-25**, 528 (1977).
- <sup>26</sup>Y. Y. Lau, K. R. Chu, L. Barnett, and V. L. Granatstein, *Int. J. Infrared Millim. Waves* **2**, 395 (1981).
- <sup>27</sup>E. Ott and W. M. Manheimer, *IEEE Trans. Plasma Sci.* **PS-3**, 1 (1975).
- <sup>28</sup>G. S. Nusinovich, W. Chen, and V. L. Granatstein, *Phys. Plasmas* **8**, 631 (2001).
- <sup>29</sup>G. S. Nusinovich, M. Walter, and J. Zhao, *Phys. Rev. E* **58**, 6594 (1998).
- <sup>30</sup>H. R. Johnson, *Proc. IRE* **43**, 684 (1955).
- <sup>31</sup>V. L. Bratman and M. A. Moiseev, *Radiophys. Quantum Electron.* **18**, 772 (1975).
- <sup>32</sup>J. M. Wachtel and E. J. Wachtel, *Appl. Phys. Lett.* **37**, 1059 (1980).
- <sup>33</sup>C. S. Kou, *Phys. Plasmas* **1**, 3093 (1994).
- <sup>34</sup>A. V. Gaponov and V. K. Yulpatov, *Radio Eng. Electron. Phys.* **12**, 582 (1967).
- <sup>35</sup>A. V. Gaponov, *Sov. Phys. JETP* **12**, 232 (1961).
- <sup>36</sup>K. R. Chu and J. Hirshfield, *Phys. Fluids* **21**, 461 (1978).